

Constraining Axion Dark Matter with Galactic-Centre Resonant Dynamics

Yonadav Barry Ginat^{1,2,*} and Bence Kocsis^{1,3}

¹*Rudolf Peierls Centre for Theoretical Physics, University of Oxford,
Parks Road, Oxford, OX1 3PU, United Kingdom*

²*New College, Holywell Street, Oxford, OX1 3BN, United Kingdom*

³*St. Hugh's College, St. Margaret's Road, Oxford, OX2 6LE, United Kingdom*

We study the influence of fuzzy-dark-matter cores on the orbits of stars at the Galactic centre. This dark matter candidate condenses into dense, solitonic cores, and, if a super-massive black hole is present at the centre of such a core, its central part forms a ‘gravitational atom’. Here, we calculate the atom’s contribution to the gravitational potential felt by a Galactic-centre star, for a general state of the atom. We study the angular-momentum dynamics this potential induces, and show that it is similar to vector resonant relaxation. Its influence is found to be potentially sufficiently strong that such a dynamical component should be accounted for in Galactic-centre modelling. For the Milky Way, the atom is expected to have some spherical asymmetry, and we use this to derive a stability condition for the disc of young, massive stars at the Galactic centre—if the atom’s mass is too large, then the disc would be destroyed. Thus, the existence of this disc constrains the mass of the particles comprising the solitonic core. We study an example model of the core, where all of the rotation of the core’s inner region is assumed to come from an $l = 1$ state, and its amplitude is determined by the halo’s spin parameter; such a core is found to be in tension with the stability of the clockwise stellar disc for $4.2 \times 10^{-20} \text{ eV} \leq m_a \leq 5.4 \times 10^{-20} \text{ eV}$ at 2σ . Other core models would vary the constrained values of m_a somewhat. These constraints will tighten significantly with future, improved data.

Introduction. Fuzzy dark matter (FDM), made of axions (or axion-like particles), is a leading candidate for a dark-matter constituent particle [1–8]. As these particles are bosons, the dark-matter haloes they form are Bose–Einstein condensates [8–10], and the axions all inhabit a single profile, with an extremely large occupation number, over astrophysical scales. An FDM halo, therefore, is characterised by a single field ψ (normalised by $\int |\psi|^2 d^3x = 1$), which solves the Schrödinger–Poisson system in the non-relativistic limit [e.g. 4, 8].

In this paper, we study potential constraints on the existence of FDM, from the long-term dynamics of stars at the Galactic centre, in particular from the dynamics of angular momenta of young, massive stars that lie in a disc around the super-massive black hole (SMBH) there [11–16], which are governed by vector resonant relaxation (VRR) [17–28]. This process is driven by the orbit-averaged torques between stars that execute rapid, eccentric orbits around the SMBH and undergo fast in-plane apsidal precession (due to the spherical component of the mass distribution) on time-scales of $10\text{--}10^3$ and $\sim 10^4$ years, respectively. VRR governs the distribution of stellar orbital directions at the Galactic centre (e.g. the clockwise disc and the counter-clockwise structure [29]). To our knowledge, VRR has never been studied in the context of ultra-light dark matter; but here we demonstrate that this may probe FDM individual particle masses m_a in a range that is currently mostly unconstrained, $10^{-20} \text{ eV} \lesssim m_a \lesssim 10^{-19} \text{ eV}$, corresponding to de Broglie wave-lengths of the order of a parsec (with speeds of order of the orbital speed at the bottom of the potential well). This range lies above the mass range constrained by the Ly α forest [$m_a \lesssim 2 \times 10^{-20} \text{ eV}$; 30] or

dwarf galaxies [$m_a \lesssim 2 \times 10^{-21} \text{ eV}$; 31, 32], but below the masses best constrained by the precession of the orbit of S2 [$10^{-19} \text{ eV} \lesssim m_a \lesssim 10^{-18} \text{ eV}$; 33–37].¹

Interestingly, VRR has an effective Hamiltonian similar to that of liquid crystals, because the stars cover axisymmetric annuli as they orbit the SMBH, whose orbit-averaged Newtonian gravitational effect is similar to the interaction between axisymmetric liquid-crystal molecules. The observed distribution of angular-momentum vectors of stars in the innermost 0.5 pc of the Galactic centre exhibits coherent and incoherent structures [13, 14, 16], possibly related to nematic-isotropic phase-transitions [20, 41].

We examine how fuzzy dark matter affects this picture. We focus on stars that orbit the SMBH in a disc of radius ~ 0.1 pc—of the same order as the de Broglie wave-length of the tentative axions—and whose mass is estimated to be a few thousand solar masses [14, 42]. We show below that a fuzzy dark-matter halo leads to the formation of a rotating dynamical component of axions of comparable mass around the SMBH, within the inner parsec, and that these axions exert torques on stars at the Galactic nucleus; that is, this extra rotating component, if indeed dark matter is primarily fuzzy, plays an important role in the dynamics of the Galactic centre, and has potential observational consequences. We derive a general framework for computing these torques, and for gauging their

¹ Other works explored the effects of dynamical friction on the relaxation of the SMBH [e.g. 4, 38, 39]; dynamical friction affects the evolution of the angular-momentum vectors much less than VRR, which is a hundredfold more efficient [23, 40].

influence on the stability of dynamical structures. As an example we show that for certain values of m_a and certain FDM field-configurations, they could even destroy the young stellar disc—and the disc’s existence could thus be used to place constraints on FDM. These constraints complement existing ones [e.g. 30, 33, 35, 43–49] [see 4, 6, 8, 50, for reviews] and are expected to improve as Galactic centre observations improve.

Fuzzy-dark-matter properties. Haloes of fuzzy dark matter are known to form dense soliton cores at their centres [4, 6, 10, 51], where the density $\rho \propto |\psi|^2$ is uniform, whose masses M_c and radii R_c are correlated with the entire halo’s virial mass M_{vir} , *viz.*,

$$R_c = 100 \text{ pc} \times \left(\frac{10^9 M_\odot}{M_c} \right) \left(\frac{10^{-22} \text{ eV}}{m_a} \right)^2, \quad (1)$$

$$M_c = 6.7 \times 10^7 M_\odot \times \left(\frac{10^{-22} \text{ eV}}{m_a} \right) \left(\frac{M_{\text{vir}}}{10^{10} M_\odot} \right)^{1/3}. \quad (2)$$

An axion core would serve as a source of dark matter at the centre of the halo. Thus, around the SMBH, such a concentration of axions would simply form a ‘gravitational atom’ [e.g. 52, 53], which, in the non-relativistic limit, has the same eigenstates as the hydrogen atom [54]. This gravitational atom is parameterised by two quantities: the total atom mass, M_a , and the Bohr radius

$$r_B \equiv \frac{\hbar^2}{GM_\bullet m_a^2}. \quad (3)$$

Suppose that r_B is of the order of a parsec, so that it encompasses the orbits of stars in the Galaxy’s inner region, and consider a star of mass m_s inside the SMBH’s gravitational sphere of influence. Then, the SMBH dominates the gravitational field, and the star’s orbit is well-approximated by a Keplerian ellipse. Further assume that

$$m_s \ll M_a \ll M_\bullet. \quad (4)$$

where $M_\bullet \approx 4 \times 10^6 M_\odot$ is the SMBH mass [55–60]. Then, to leading order, the force the atom would exert on a star (a classical object) is generated by a potential

$$\Phi(\mathbf{x}) = - \int d^3 y \frac{G \rho_a(\mathbf{y})}{|\mathbf{x} - \mathbf{y}|}, \quad (5)$$

where $\rho_a(\mathbf{y}) \equiv M_a |\psi(\mathbf{y})|^2$, with ψ being the field configuration of the gravitational atom. Generically, ψ is a linear combination of hydrogen-atom eigenstates $|nlm\rangle$ for the usual quantum numbers n, l, m ,

$$|\psi\rangle = \sum_{n,l,m} \alpha_{nlm} |nlm\rangle. \quad (6)$$

Orbit averaging. The hierarchy (4) implies that the dynamics are, to leading order, decoupled Kepler problems (both for the axions and the star); their interaction occurs on longer time-scales than the orbital times, and therefore one may orbit-average their interaction Hamiltonian (5). The interaction of orbit-averaged Keplerian ellipses is governed by resonant relaxation [17–19, 21, 24, 25, 61], so we require the orbit-averaged value of Φ , over a Keplerian orbit of the star around the SMBH. This orbit, described by the co-ordinate \mathbf{x} , is assumed to have orbital parameters a, e, i, Ω, ω , denoting the semi-major axis, eccentricity, inclination and the arguments of the ascending node and the pericentre, respectively. The orbit-dependent part of equation (5) is $|\mathbf{x} - \mathbf{y}|^{-1}$ (where \mathbf{y} is itself an integration variable); we decompose it with spherical harmonics as

$$\frac{1}{|\mathbf{x} - \mathbf{y}|} = \sum_{l,m} \frac{4\pi}{2l+1} \frac{\min\{x, y\}^l}{\max\{x, y\}^{l+1}} Y_{lm}^*(\hat{\mathbf{x}}) Y_{lm}(\hat{\mathbf{y}}), \quad (7)$$

where $x = |\mathbf{x}|$, $\hat{\mathbf{x}} = \mathbf{x}/x$, *etc.* We time-average over all effects that take place on time-scales much shorter than those of orbital energy change, eccentricity change, and the change of orbital orientation driven by VRR, which takes place on megayear time-scales [18, 19]. In particular, the mean anomaly and the argument of pericentre change rapidly, and one may average over them. We calculate the double-averaged potential $\langle \Phi \rangle_{\text{da}}$, over of these angles, in the appendix. The result is

$$\langle \Phi \rangle_{\text{da}} = - \sum_{l,m} J_{lm} Y_{lm}^*(\hat{\mathbf{L}}), \quad (8)$$

where the coefficients J_{lm} are defined in the appendix (equation (37)), and the chosen $\hat{\mathbf{z}}$ -axis for the multipole decomposition is $\hat{\mathbf{L}}_a$, the direction of the atom’s angular momentum, and \mathbf{L} is the star’s angular momentum.

Equation (37) implies, *inter alia*, that, if $|\psi\rangle = \sum \alpha_{n_0 l_0 m_0} |n_0 l_0 m_0\rangle$ is a super-position of non-degenerate eigenstates (i.e. contains only at most one eigenstate with each n_0), then $J_{lm} = 0$ unless $m = 0$. Indeed, for this state the behaviour of this potential is quite similar to that of the classical case, where one may write

$$\langle \Phi \rangle_{\text{da}} = - \sum_{l_0} \sum_{l=0}^{2l_0} J_{l,l_0} P_l(\hat{\mathbf{L}} \cdot \hat{\mathbf{L}}_a), \quad (9)$$

where $\sqrt{4\pi/(2l+1)} J_{l,l_0} = \sum_{l_0} J_{l,l_0}$, with the contribution of the mode $|n_0 l_0 m_0\rangle$ denoted by $J_{l,l_0} \propto |\alpha_{n_0 l_0 m_0}|^2$. This potential induces precession about $\hat{\mathbf{L}}_a$, given by

$$\begin{aligned} \boldsymbol{\Omega} &= -m_s \sum_{l_0} \sum_{l=0}^{2l_0} \frac{J_{l,l_0}}{L} P'_l(\hat{\mathbf{L}} \cdot \hat{\mathbf{L}}_a) \hat{\mathbf{L}}_a \\ &= -\frac{GM_a m_s}{L r_B} \sum_{l_0,l} I_{l,l_0} P'_l(\hat{\mathbf{L}} \cdot \hat{\mathbf{L}}_a) \hat{\mathbf{L}}_a, \end{aligned} \quad (10)$$

and in general

$$\boldsymbol{\Omega} = -\frac{m_s}{L} \sum_{lm} J_{lm} \frac{\partial Y_{lm}^*(\hat{\mathbf{L}})}{\partial \hat{\mathbf{L}}} = -\frac{GM_a m_s}{L r_B} \sum_{lm} I_{lm} \frac{\partial Y_{lm}^*}{\partial \hat{\mathbf{L}}}, \quad (11)$$

where we have defined the dimensionless coefficients

$$I_{l,l_0} \left(\frac{a}{r_B}, e \right) \equiv \frac{r_B}{GM_a} J_{l,l_0}, \quad (12)$$

$$I_{lm} \left(\frac{a}{r_B}, e \right) \equiv \frac{r_B}{GM_a} J_{lm}.$$

Equation (11) implies that an axion core with some angular momentum would participate in the VRR dynamics of the Galactic centre, and thus must be accounted for in the latter's modelling. Let us exemplify this by calculating one aspect of the axions' influence on the nuclear stellar disc; to do so, we list some assumptions and estimates of the relevant parameters below, starting with the clockwise disc.

Resonant disc-breaking. The distribution of young, massive stars at the Galactic centre consists of an inner disc, rotating clockwise, whose mass is $3000 M_\odot \lesssim M_d \lesssim 10^4 M_\odot$, up to a radius of ~ 0.4 pc, and an outer, tilted disc, whose inner radius is ~ 0.4 pc [13, 14, 16, 42].

Having computed the potential that the gravitational atom induces, we can use it to calculate the effect that it would have on a disc of stars. Equation (10) applies to every individual star in the disc, but they also feel the torques from all the other stars. Thus, whether a given star remains bound to the disc, is determined by the relative strength of the torque exerted on it by the rest of the disc, versus the gravitational atom's torque-difference within the disc. Recently, ref. [62] derived a stability criterion for a disc under the influence of a potential like (9) by considering the tidal torque (in angular-momentum space) due to the external potential, and comparing it with the torque from the rest of the disc: if the disc, due to its thickness, has width $\Delta \mathbf{L}$ in angular-momentum space, about the total \mathbf{L}_d , then it is stable if

$$\left| \left(\Delta L \frac{\partial \boldsymbol{\Omega}}{\partial L} \times \hat{\mathbf{L}} + \frac{1}{L} \boldsymbol{\Omega} \times \Delta \mathbf{L} \right) \cdot \Delta \hat{\mathbf{L}} \right| < \left| \boldsymbol{\Omega}_d \times \hat{\mathbf{L}} \right|, \quad (13)$$

where $\boldsymbol{\Omega}_d$ is the frequency of precession of the angular momenta of the disc stars, about \mathbf{L}_d , and $\Delta \hat{\mathbf{L}} \equiv \Delta \mathbf{L} / \Delta L$. The disc's thickness $\Delta L / L$ is related to its maximum opening half-angle ι as $\Delta L / L \sim 2 \sin \iota$, and satisfies $\iota < \theta$; its precession frequency is [19, 25]

$$\boldsymbol{\Omega}_d = -\sum_{l=2}^{\infty} \sum_{i \in \text{disc}} \frac{\mathcal{J}_{isl}}{L} P_l'(\hat{\mathbf{L}} \cdot \hat{\mathbf{L}}_i) \hat{\mathbf{L}}_i, \quad (14)$$

where \mathcal{J}_{isl} are defined in [19]. Parameterising the right-hand side of inequality (13) without loss of generality as $[Gm_s M_d / (L a_d)] \xi_d \sin \iota$, where, roughly, ξ_d is of order

unity, one needs to have, for stability,

$$\left| \sum_{lm} \sum_{n \in \{x,y,z\}} \frac{J_{lm}}{GM_d} \Delta L_n \left(\frac{\partial^2 Y_{lm}^*}{\partial \hat{L}_n \partial \hat{\mathbf{L}}} \times \hat{\mathbf{L}} \right) \cdot \Delta \hat{\mathbf{L}} \right| < \frac{\xi_d}{a_d}, \quad (15)$$

where ΔL_n is the n th Cartesian component of $\Delta \mathbf{L}$. This holds for any $\Delta \mathbf{L} \perp \mathbf{L}_d$, whose magnitude is $\Delta L = 2L \sin \iota$. For the case of equation (9), this reduces to

$$\left| \sum_{l,l_0} \frac{2J_{l,l_0}}{GM_d} P_l''(\hat{\mathbf{L}} \cdot \hat{\mathbf{L}}_a) \sin^2 \theta \right| < \frac{\xi_d}{a_d}, \quad (16)$$

where J_{l,l_0} is defined below equation (9), $\cos \theta = \hat{\mathbf{L}}_d \cdot \hat{\mathbf{L}}_a$, and the direction of $\Delta \mathbf{L}$ which maximises the left-hand side is in the plane spanned by \mathbf{L}_d and \mathbf{L}_a . Inequalities (15–16) are the main theoretical result of this paper, and describe the disc's stability under the influence of any FDM configuration, and will apply to any nuclear stellar discs, including in other galaxies.

Rotating core. Let us now apply the above result to a specific model of the FDM core, which we motivate below. For a given axion core, one can approximate the mass of the gravitational atom [63, 64] as the mass enclosed in a sphere whose radius is the minimum between R_c and the radius of influence of the SMBH, GM_\bullet / σ^2 , where $\sigma \approx 100 \text{ km s}^{-1}$ is the velocity dispersion of the nuclear cluster [65], that is,

$$M_a \approx M_{a,\text{exp}} \equiv M_c \left(\frac{\min \{GM_\bullet / \sigma^2, R_c\}}{R_c} \right)^3. \quad (17)$$

Let us proceed to estimate the gravitational atom's shape, for $m_a \leq 10^{-18} \text{ eV}$. Generically, the core of an FDM halo should retain some rotation, because the halo should have some angular momentum, which can be encapsulated by the spin parameter $\lambda \equiv L_h |E|^{1/2} / (GM_{\text{vir}}^{5/2})$, where E is the binding energy of the halo [e.g. 66, 67].² With it, one can relate the global FDM halo properties to the rotation of the axion core (and hence the atom): one can define the parameter

$$\alpha \equiv \|\Pi_{l \neq 0} |\psi\rangle\| \sqrt{\frac{M_a}{M_{a,\text{exp}}}}, \quad (18)$$

where $\Pi_{l \neq 0}$ is an orthogonal projection on the $l \neq 0$ subspace, M_a is the atom's mass, and $M_{a,\text{exp}}$ is the value expected for it, i.e. the one obtained from equations (1–2) and (17). α thus quantifies the 'rotating mass' of the

² One may bound λ from above by a quantum-mechanical (loose) version of Sundman's inequality, $\left| \sum_{ijk} \varepsilon_{ijk} \langle \psi | x^j p^k | \psi \rangle \right|^2 \leq 6 \langle \psi | x^2 | \psi \rangle \langle \psi | p^2 | \psi \rangle$ combined with the virial theorem.

FDM atom, given by $|\alpha|^2 M_{a,\text{exp}}$. It is, strictly speaking, a free parameter of the model (physically determined by the intricate details of the atom's formation process).

We now give an argument for a plausible value for α , but later we treat it as an additional parameter and infer constraints on the pair (m_a, α) . If $M_a = M_{a,\text{exp}}$, the gravitational atom's wave-function (6) satisfies

$$|\alpha|^2 = \sum_{n,l \neq 0,m} |\alpha_{nlm}|^2. \quad (19)$$

For the core, one would have $\langle L_a \rangle \equiv M_c/m_a \langle \psi | L_a | \psi \rangle = GM_c^{5/2} \lambda_c / \sqrt{|E_c|}$, where λ_c denotes the core's spin parameter; this allows one to gauge α as follows. We assume that, energetically, the Bose-Einstein condensate would settle onto the lowest-energy states, subject to the constraint of fixed angular momentum $\langle L_a \rangle = GM_c^{5/2} \lambda_c / \sqrt{|E_c|}$. We argue in the appendix why, based on energy arguments, it is plausible to take

$$|\psi\rangle \approx \alpha_{100} |100\rangle + \alpha_{211} |211\rangle \quad (20)$$

for the field configuration of the gravitational atom, where $|\alpha_{100}|$, and $|\alpha_{211}|$ are fixed by the above requirement on angular momentum. While the state (20) is simple, the formalism developed here allows one to study the interaction of the atom with the disc for any ψ . Thus, λ_c determines α by

$$|\alpha|^2 = \lambda_c \sqrt{\frac{10}{3}} \frac{m_a \sqrt{GM_c R_c}}{\sqrt{l_0(l_0+1)} \hbar} \approx 8.4 \times 10^{-2} \left(\frac{\lambda_c}{0.06} \right); \quad (21)$$

here, the m_a -dependence drops, and we have used $|E| = \frac{3GM_c^2}{10R_c}$ for a uniform, virialised core, and $L_a = \hbar |\alpha|^2 \sqrt{l_0(l_0+1)} M_c/m_a$ with $l_0 = 1$.³ For our model of α we assume that it is given by equation (21) with $|\psi\rangle$ given by (20), with the additional input that $\lambda_c = \lambda_{\text{halo}}$ [cf. 68]. For the Milky Way, λ_{halo} is estimated to be $\lambda_{\text{halo}} \approx 0.05\text{--}0.09$ [69], so here we use $\lambda_c \approx 0.05\text{--}0.09$.⁴ The angle between the angular-momentum vector of the nuclear inner disc and the rotation direction of the Galactic disc, which we assume to be aligned with the halo and hence with $\hat{\mathbf{L}}_a$, is approximately $\theta \approx 79^\circ$ [13, 16].

The state $|211\rangle$ is also unstable to the super-radiant instability [72–74], and also potentially susceptible to accretion into the SMBH. We show in the appendix that

³ This could be relaxed to $L_a = \hbar |\alpha|^2 m_0 M_c/m_a$, with $m_0 = 1$, if the angular-momentum vector is aligned with the $\hat{\mathbf{z}}$ -axis, but to be more conservative we keep the additional $\sqrt{2}$ factor.

⁴ Ref. [69] estimated $\lambda' \equiv L_h / [\sqrt{2} M_{\text{vir}} R_h V_{\text{circ}}(R_h)]$, rather than λ , to be $0.061^{+0.022}_{-0.016}$. λ' is smaller than λ_{halo} by a function of the concentration [67, 70]; for a halo concentration of 10 [71] (before disc formation and halo contraction), this implies that $\lambda = 1.12\lambda'$, which is what we use.

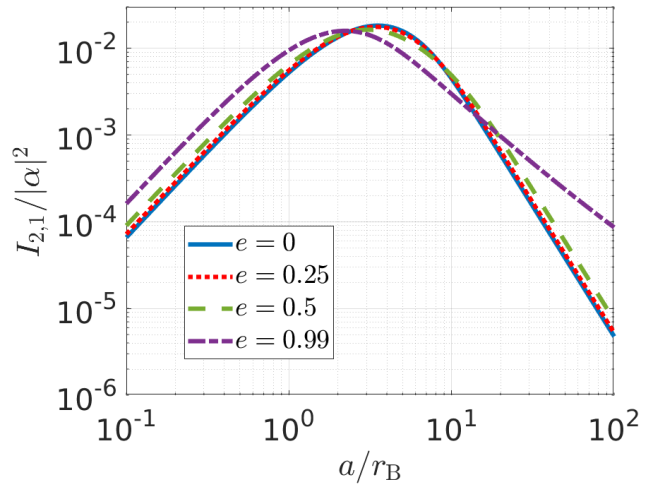


FIG. 1. The integral $I_{2,1}$ as a function of the semi-major axis, plotted for various eccentricities, for the wave-function (20).

neither of these phenomena is relevant for masses considered here.

In summary, we assumed that (i) $|\psi\rangle$ is well-approximated by equation (20) (justified by energy considerations), (ii) $M_a = M_{a,\text{exp}}$, (iii) $\lambda_c = \lambda$, and (iv) the value of λ . By making α a free parameter, it absorbs the modelling assumptions (ii–iv) on its mass and angular momentum (and consequently the relation between λ and λ_c), which are thus relaxed.

For the state (20) equation (9) becomes

$$\langle \Phi \rangle_{\text{da}} = \sum_{l_0=0}^1 \sum_{l=0}^{2l_0} J_{l,l_0} P_l(\hat{\mathbf{L}} \cdot \hat{\mathbf{L}}_a), \quad (22)$$

and by equations (12) and (37),

$$I_{0,0} = 4\sqrt{2} [1 - |\alpha|^2] \int_0^\infty \frac{y^2 e^{-2y/r_B} s_0(a, y, e, 0)}{r_B^2 \max\{a, y\}} dy, \quad (23)$$

$$I_{2,1} = \frac{|\alpha|^2}{240 r_B^4} \int_0^\infty \frac{y^4 s_2(a, y, e, 0)}{e^{y/r_B} \max\{a, y\}} \left[\frac{\min\{a, y\}}{\max\{a, y\}} \right]^2 dy, \quad (24)$$

and the rest of J_{l,l_0} are zero or negligible. $I_{2,1}$ is plotted in Figure 1. The monopole term, $J_{0,0}$, sources mass precession of the pericentre by the density profile $\rho_a = M_a |\psi|^2$, while the quadrupole, $J_{2,1}$ is a VRR interaction.

The potential (22) drives the precession of $\hat{\mathbf{L}}$ about the $\hat{\mathbf{z}}$ -axis, i.e. about $\hat{\mathbf{L}}_a$, with frequency [19]

$$\Omega = -3m_s \frac{J_{2,1}}{L} (\hat{\mathbf{L}} \cdot \hat{\mathbf{L}}_a) \hat{\mathbf{L}}_a. \quad (25)$$

Parameter	Value	Ref.
M_{vir}	$(1.1 \pm 0.1) \times 10^{12} M_{\odot}$	[76]
M_{d}	$(6500 \pm 3500) M_{\odot}$	[12, 14, 42]
ι (option 1)	$14^{\circ} \pm 4^{\circ}$	[12]
ι (option 2)	$16^{\circ} \pm 4.8^{\circ}$	[13, 16]
λ	0.067 ± 0.018	[69]

TABLE I. Adopted parameter values and 1σ uncertainties.

Constraints from disc stability. For the case of the wave-function (20), equation (16) becomes

$$|\alpha|^2 M_{\text{a,exp}} < M_{\text{d}} \frac{r_{\text{B}} \xi_{\text{d}} |\alpha|^2}{a_{\text{d}} 6 I_{2,1} |\sin^2 \theta|}. \quad (26)$$

If the disc is unstable, we estimate its disruption time to be Ω_{d}^{-1} [62], which is less than 10 Myr for $m_{\text{a}} \in [3, 7] \times 10^{-20}$ eV (for the mean values of the parameters).

The constraint (26) is plotted in figure 2; parameter values are specified in table I. Here, we have used a disc whose semi-major-axis distribution is $dN/da \propto a^{-3/4}$, the eccentricities are uniformly distributed, and the inclinations are normally-distributed with a variance ι . We consider two possibilities for its value: $\iota = 14^{\circ} \pm 4^{\circ}$ [12] (a conservative value) and $\iota = 16^{\circ}$, preferred by recent observations [13, 16],⁵ where we estimate the error as 4.8° ;⁶ The test star s is placed at semi-major axes $a \in [0.03, 0.4]$ pc, with $\hat{\mathbf{L}} \cdot \hat{\mathbf{L}}_{\text{d}} = \cos \iota$. Here, ξ_{d} is calculated for each value of a directly from equation (14), and for concreteness we used 648 particles in the disc, normalised to have a total disc mass $M_{\text{d}} = \sum_{i=1}^{648} m_i$, with equal masses.⁷ The red line in figure 2 is the expected value of $|\alpha|^2 M_{\text{a}}$ based on the parameters described above, while the blue line corresponds to the value of $|\alpha|^2 M_{\text{a}}$ saturating inequality (26), minimised over all semi-major axes of the test star. Uncertainties resulting from the errors in the parameters in table I are plotted as shaded regions. An axion core with a particle mass m_{a} such that the former curve lies above the latter is inconsistent with the existence of the clockwise disc at the Galactic centre, because such a disc would have been broken by the influence of the FDM atom. Figure 3 shows which semi-major axes in the disc are expected to become unstable, in an example. Propagating the uncertainties yields that this occurs at 2σ for $m_{\text{a}} \in [m_{\text{low}}, m_{\text{high}}]$,

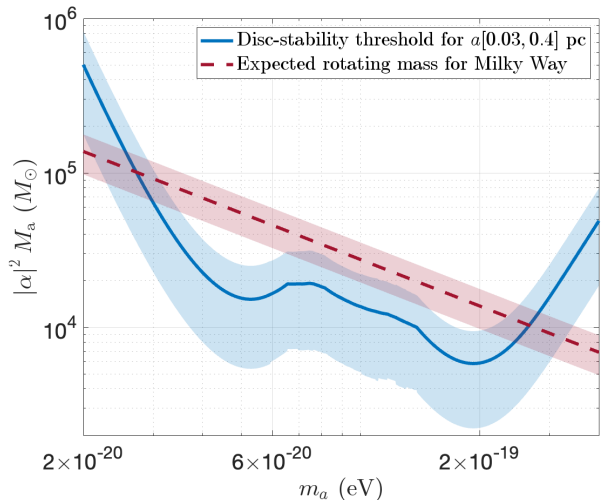


FIG. 2. The upper limit for disc stability from inequality (26), for a Galactic-centre-like disc with parameters specified in the text and table I (in blue). The expected value of the rotating mass $|\alpha|^2 M_{\text{a}}$ is plotted too (red, dashed line). The shaded regions around both curves show estimated 1σ uncertainties. The disc should be disrupted for values of m_{a} where the maximum rotating mass for disc stability is lower than $|\alpha|^2 M_{\text{a}}$, and are thus constrained.

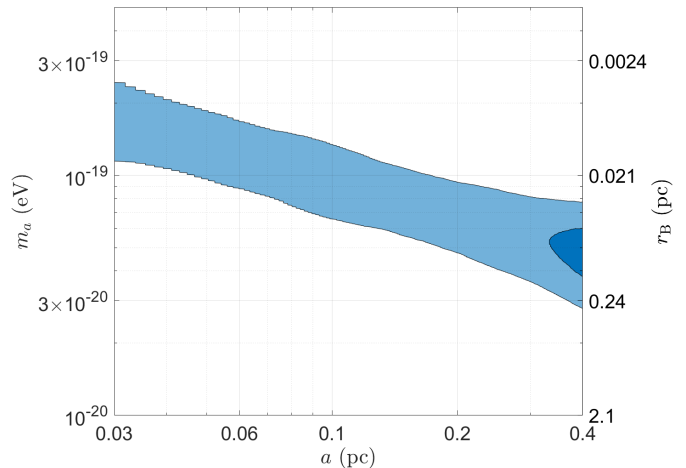


FIG. 3. The semi-major axes in the disc which the gravitational atom renders unstable. Here $M_{\text{d}} = 4000 M_{\odot}$, $\iota = 10^{\circ}$, $M_{\text{vir}} = 1.1 \times 10^{12} M_{\odot}$, and $\lambda_{\text{c}} = 0.06$; the inner, darker region corresponds to $M_{\text{d}} = 10^4 M_{\odot}$ with the same values for the other parameters.

⁵ Even if the initial inclination is smaller, it increases rapidly (within $\mathcal{O}(1)$ Myr), mostly by two-body relaxation within the disc, which is efficient in two dimensions [25, 75]; external effects like the nuclear cluster would make this even more rapid [25].

⁶ This is done by considering the fourth moment of the haversine distance (on the angular-momentum-direction sphere) between the 15 stars with known orbital parameters listed in [16], and the location of the disc's centre at $(i, \Omega) = (126^{\circ}, 104^{\circ})$ [13].

⁷ We truncated the multipole sum at $l = 120$, for accuracy [19].

where $\{m_{\text{low}}, m_{\text{high}}\} = \{4.2, 5.48\} \times 10^{-20}$ eV for the conservative choice of ι , or $\{3.82, 5.98\} \times 10^{-20}$ eV for $\iota = 16^{\circ} \pm 4.8^{\circ}$.

While these constraints did not account for the influence of the spherical nuclear cluster (which has some net angular momentum [16]), this is not expected to modify them significantly: the nuclear cluster is not aligned

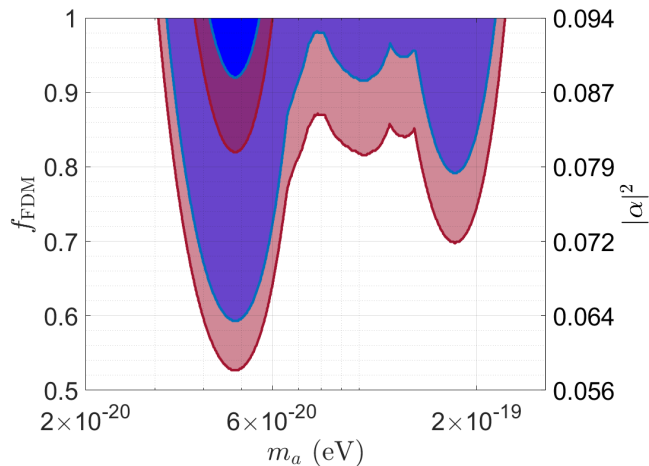


FIG. 4. Values of m_a inconsistent with a stable disc, obtained from imposing inequality (26), for various values of α (or alternatively, fixing α by equation 21, for the FDM dark-matter fraction, f_{FDM}). The shaded blue contours correspond to an opening angle $\iota = 14^\circ \pm 4^\circ$, while the red ones use $\iota = 16^\circ \pm 4.8^\circ$. The darker regions are 2σ levels, while the lighter ones delineate 1σ regions, for the field configuration described in the text.

with the clockwise disc [65, 77], so if $m \in [m_{\text{low}}, m_{\text{high}}]$, the atom alone breaks the disc and the nuclear cluster could not stabilise the disc—only destabilise it further. On the other hand, if $m_a \gg m_{\text{high}}$ —and hence $M_{a,\text{exp}} \ll M_d$ —then it is possible that $\hat{\mathbf{L}}_a$ would be rotated to align itself with \mathbf{L}_d , by resonant dynamical friction [23, 26]; this, again, does not invalidate the conclusion for $m \in [m_{\text{low}}, m_{\text{high}}]$. A full, detailed treatment of these situations is deferred for future work.

Generalising the dark-matter model to a case where only a fraction f_{FDM} of dark matter is fuzzy (and the rest is described by another model), one can generalise the derivation in this paper to derive a constraint on m_a and f_{FDM} . Assuming that the dark-matter core equations (1–2) continue to hold, $M_a \propto f_{\text{FDM}}^{4/3}$, while equation (21) and inequality (26) are unchanged, we show in figure 4 the corresponding constraint, generalising figure 2. One can absorb f_{FDM} into α , by transforming $\alpha \mapsto \alpha f_{\text{FDM}}^{2/3}$, and then the contours in this figure can be construed as constraints on α —because the right-hand side of (26) is independent of both α and f_{FDM} . This is therefore a way of incorporating uncertainties in equation (21) and possible deviations from equations (2) and (17) into our analysis. By treating α as a free parameter, the stability of the disc only implies a joint constraint on the pair (m_a, α) , via equation (26).⁸ In this light, equation (21)

⁸ Uncertainties in θ can also be absorbed into α by a re-definition $\alpha \mapsto \alpha \sqrt{|\sin^2 \theta / \sin^2 79^\circ|}$.

can be viewed as a theoretical model for α , which can break the degeneracy.

Conclusions. In this letter, we showed that the dynamics of the Galactic centre are strongly influenced by ultra-light axions, which cannot be neglected in the dynamical modelling of the stellar distribution there—if these particles indeed constitute a sizeable fraction of dark matter. We calculated the gravitational torque they exert on stars, for a general axion-core state. We found that their influence is so strong, that under plausible assumptions on the rotation rate of the core and the gravitational atom’s wave-function, these torques are should destabilise—or possibly break—the disc of young, massive stars. Given the observed properties of these stars in the Galactic centre, this imposes a stringent constraint on the allowed range of particle masses for the axions comprising this core, for the model studied here. Treating α as a free parameter to be constrained, allows one to relax many of the modelling assumptions, and incorporate them into the parameter α , thereby producing 2-dimensional constraints on (m_a, α) . These constraints will improve with better Galactic centre data—especially when the uncertainties in the parameters in table I are reduced—and also potentially with observations of nuclear discs in other galaxies.

Acknowledgements. We are grateful to Kfir Blum, Sebastiano von Fellenberg, Pedro Ferreira, Sofia Flores, Chris Hamilton, John Magorrian and Taras Panamarev for helpful discussions. This work was supported by the Science and Technology Facilities Council grant No. ST/W000903/1, and by a Leverhulme Trust International Professorship Grant (No. LIP-2020-014). Y.B.G. was partly supported by the Simons Foundation via a Simons Investigator Award to A.A. Schekochihin.

* yb.ginat@physics.ox.ac.uk

- [1] L. F. Abbott and P. Sikivie, A cosmological bound on the invisible axion, *Physics Letters B* **120**, 133 (1983).
- [2] M. Dine and W. Fischler, The not-so-harmless axion, *Physics Letters B* **120**, 137 (1983).
- [3] J. Preskill, M. B. Wise, and F. Wilczek, Cosmology of the invisible axion, *Physics Letters B* **120**, 127 (1983).
- [4] L. Hui, J. P. Ostriker, S. Tremaine, and E. Witten, Ultra-light scalars as cosmological dark matter, *Phys. Rev. D* **95**, 043541 (2017), arXiv:1610.08297 [astro-ph.CO].
- [5] B. Bar-Or, J.-B. Fouvry, and S. Tremaine, Relaxation in a Fuzzy Dark Matter Halo, *ApJ* **871**, 28 (2019), arXiv:1809.07673 [astro-ph.GA].
- [6] L. Hui, Wave Dark Matter, *ARA&A* **59**, 247 (2021), arXiv:2101.11735 [astro-ph.CO].
- [7] B. Bar-Or, J.-B. Fouvry, and S. Tremaine, Relaxation in a Fuzzy Dark Matter Halo. II. Self-consistent Kinetic Equations, *ApJ* **915**, 27 (2021), arXiv:2010.10212 [astro-ph.GA].
- [8] D. J. E. Marsh, D. Ellis, and V. M. Mehta, *Dark Matter: Evidence, Theory, and Constraints* (Princeton University

- Press, Princeton, N.J., 2024).
- [9] H.-Y. Schive, T. Chiueh, and T. Broadhurst, Cosmic structure as the quantum interference of a coherent dark wave, *Nature Physics* **10**, 496 (2014), arXiv:1406.6586 [astro-ph.GA].
- [10] H.-Y. Schive, M.-H. Liao, T.-P. Woo, S.-K. Wong, T. Chiueh, T. Broadhurst, and W. Y. P. Hwang, Understanding the Core-Halo Relation of Quantum Wave Dark Matter from 3D Simulations, *Phys. Rev. Lett.* **113**, 261302 (2014), arXiv:1407.7762 [astro-ph.GA].
- [11] Y. Levin and A. M. Beloborodov, Stellar Disk in the Galactic Center: A Remnant of a Dense Accretion Disk?, *ApJL* **590**, L33 (2003), astro-ph/0303436.
- [12] T. Paumard, R. Genzel, F. Martins, S. Nayakshin, A. M. Beloborodov, Y. Levin, S. Trippe, F. Eisenhauer, T. Ott, S. Gillessen, *et al.*, The Two Young Star Disks in the Central Parsec of the Galaxy: Properties, Dynamics, and Formation, *ApJ* **643**, 1011 (2006), astro-ph/0601268.
- [13] H. Bartko, F. Martins, T. K. Fritz, R. Genzel, Y. Levin, H. B. Perets, T. Paumard, S. Nayakshin, O. Gerhard, T. Alexander, *et al.*, Evidence for Warped Disks of Young Stars in the Galactic Center, *ApJ* **697**, 1741 (2009), arXiv:0811.3903 [astro-ph].
- [14] S. Yelda, A. M. Ghez, J. R. Lu, T. Do, L. Meyer, M. R. Morris, and K. Matthews, Properties of the Remnant Clockwise Disk of Young Stars in the Galactic Center, *ApJ* **783**, 131 (2014), arXiv:1401.7354 [astro-ph.GA].
- [15] Schödel, R., Noguera-Lara, F., Gallego-Cano, E., Shahzamanian, B., Gallego-Calvente, A. T., and Gardini, A., The milky way's nuclear star cluster: Old, metal-rich, and cuspy—structure and star formation history from deep imaging, *A&A* **641**, A102 (2020).
- [16] S. D. von Fellenberg, S. Gillessen, J. Stadler, M. Bauböck, R. Genzel, T. de Zeeuw, O. Pfuhl, P. Amaro Seoane, A. Drescher, F. Eisenhauer, *et al.*, The Young Stars in the Galactic Center, *ApJ* **932**, L6 (2022), arXiv:2205.07595 [astro-ph.GA].
- [17] K. P. Rauch and S. Tremaine, Resonant relaxation in stellar systems, *New A* **1**, 149 (1996), arXiv:astro-ph/9603018 [astro-ph].
- [18] B. Kocsis and S. Tremaine, Resonant relaxation and the warp of the stellar disc in the Galactic Centre, *MNRAS* **412**, 187 (2011), arXiv:1006.0001 [astro-ph.GA].
- [19] B. Kocsis and S. Tremaine, A numerical study of vector resonant relaxation, *MNRAS* **448**, 3265 (2015), arXiv:1406.1178 [astro-ph.GA].
- [20] Z. Roupas, B. Kocsis, and S. Tremaine, Isotropic-Nematic Phase Transitions in Gravitational Systems, *ApJ* **842**, 90 (2017), arXiv:1701.03271 [astro-ph.GA].
- [21] B. Bar-Or and J.-B. Fouvry, Scalar Resonant Relaxation of Stars around a Massive Black Hole, *ApJ* **860**, L23 (2018), arXiv:1802.08890 [astro-ph.GA].
- [22] J.-B. Fouvry, B. Bar-Or, and P.-H. Chavanis, Vector Resonant Relaxation of Stars around a Massive Black Hole, *ApJ* **883**, 161 (2019), arXiv:1812.07053 [astro-ph.GA].
- [23] Á. Szölgvény, G. Máthé, and B. Kocsis, Resonant Dynamical Friction in Nuclear Star Clusters: Rapid Alignment of an Intermediate-mass Black Hole with a Stellar Disk, *ApJ* **919**, 140 (2021), arXiv:2103.14042 [astro-ph.GA].
- [24] J.-B. Fouvry, W. Dehnen, S. Tremaine, and B. Bar-Or, Secular Dynamics around a Supermassive black hole via Multipole Expansion, *ApJ* **931**, 8 (2022), arXiv:2011.01673 [astro-ph.GA].
- [25] T. Panamarev and B. Kocsis, A numerical study of stellar discs in galactic nuclei, *MNRAS* **517**, arXiv:2207.06398 (2022), arXiv:2207.06398 [astro-ph.GA].
- [26] Y. B. Ginat, T. Panamarev, B. Kocsis, and H. B. Perets, Resonant dynamical friction around a supermassive black hole: analytical description, *MNRAS* **525**, 4202 (2023), arXiv:2211.14784 [astro-ph.GA].
- [27] H. Wang and B. Kocsis, Anisotropic mass segregation: Two-component mean-field model, *Phys. Rev. D* **108**, 103004 (2023), arXiv:2302.12842 [astro-ph.GA].
- [28] S. Flores and J.-B. Fouvry, Vector resonant relaxation and statistical closure theory: Direct interaction approximation, *Phys. Rev. E* **111**, 044111 (2025), arXiv:2406.19306 [astro-ph.GA].
- [29] R. Genzel, F. Eisenhauer, and S. Gillessen, The Galactic Center massive black hole and nuclear star cluster, *Reviews of Modern Physics* **82**, 3121 (2010), arXiv:1006.0064 [astro-ph.GA].
- [30] K. K. Rogers and H. V. Peiris, Strong Bound on Canonical Ultralight Axion Dark Matter from the Lyman-Alpha Forest, *Phys. Rev. Lett.* **126**, 071302 (2021), arXiv:2007.12705 [astro-ph.CO].
- [31] A. A. El-Zant, Z. Roupas, and J. Silk, Ejection of supermassive black holes and implications for merger rates in fuzzy dark matter haloes, *MNRAS* **499**, 2575 (2020), arXiv:2009.10167 [astro-ph.GA].
- [32] T. Zimmermann, J. Alvey, D. J. E. Marsh, M. Fairbairn, and J. I. Read, Dwarf galaxies imply dark matter is heavier than $2.2 \times 10^{-21} \text{ eV}$, arXiv e-prints, arXiv:2405.20374 (2024), arXiv:2405.20374 [astro-ph.CO].
- [33] Gravity Collaboration, A. Amorim, M. Bauböck, M. Benisty, J. P. Berger, Y. Clénet, V. Coudé Du Forest, T. de Zeeuw, J. Dexter, G. Duvert, *et al.*, Scalar field effects on the orbit of S2 star, *MNRAS* **489**, 4606 (2019), arXiv:1908.06681 [astro-ph.GA].
- [34] G.-W. Yuan, Z.-Q. Shen, Y.-L. S. Tsai, Q. Yuan, and Y.-Z. Fan, Constraining ultralight bosonic dark matter with Keck observations of S2's orbit and kinematics, *Phys. Rev. D* **106**, 103024 (2022), arXiv:2205.04970 [astro-ph.HE].
- [35] A. Foschi, R. Abuter, N. Aimar, P. Amaro Seoane, A. Amorim, M. Bauböck, J. P. Berger, H. Bonnet, G. Bourdarot, Gravity Collaboration, *et al.*, Using the motion of S2 to constrain scalar clouds around Sgr A*, *MNRAS* **524**, 1075 (2023), arXiv:2306.17215 [astro-ph.GA].
- [36] R. Della Monica and I. de Martino, Bounding the mass of ultralight bosonic dark matter particles with the motion of the S2 star around Sgr A*, *Phys. Rev. D* **108**, L101303 (2023), arXiv:2305.10242 [gr-qc].
- [37] R. Della Monica and I. de Martino, Narrowing the allowed mass range of ultralight bosons with the S2 star, *A&A* **670**, L4 (2023), arXiv:2206.03980 [gr-qc].
- [38] G. Bertone, Dark matter, black holes, and gravitational waves, *Nuclear Physics B* **1003**, 116487 (2024), arXiv:2404.11513 [astro-ph.CO].
- [39] N. Glennon, N. Musoke, E. O. Nadler, C. Prescod-Weinstein, and R. H. Wechsler, Dynamical friction in self-interacting ultralight dark matter, *Phys. Rev. D* **109**, 063501 (2024), arXiv:2312.07684 [astro-ph.CO].
- [40] B. Kocsis, N. Yunes, and A. Loeb, Observable signatures of extreme mass-ratio inspiral black hole binaries embedded in thin accretion disks, *Phys. Rev. D* **84**, 024032

- (2011), arXiv:1104.2322 [astro-ph.GA].
- [41] Á. Takács and B. Kocsis, Isotropic-Nematic Phase Transitions in Gravitational Systems. II. Higher Order Multipoles, *ApJ* **856**, 113 (2018), arXiv:1712.04449 [astro-ph.GA].
- [42] H. Bartko, F. Martins, S. Trippe, T. K. Fritz, R. Genzel, T. Ott, F. Eisenhauer, S. Gillessen, T. Paumard, T. Alexander, *et al.*, An Extremely Top-Heavy Initial Mass Function in the Galactic Center Stellar Disks, *ApJ* **708**, 834 (2010), arXiv:0908.2177 [astro-ph.GA].
- [43] D. J. E. Marsh and J. C. Niemeyer, Strong Constraints on Fuzzy Dark Matter from Ultrafaint Dwarf Galaxy Eridanus II, *Phys. Rev. Lett.* **123**, 051103 (2019), arXiv:1810.08543 [astro-ph.CO].
- [44] H.-Y. Schive, T. Chiueh, and T. Broadhurst, Soliton Random Walk and the Cluster-Stripping Problem in Ultralight Dark Matter, *Phys. Rev. Lett.* **124**, 201301 (2020), arXiv:1912.09483 [astro-ph.GA].
- [45] V. Desjacques and A. Nusser, Axion core-halo mass and the black hole-halo mass relation: constraints on a few parsec scales, *MNRAS* **488**, 4497 (2019), arXiv:1905.03450 [astro-ph.CO].
- [46] M. Rozner, E. Grishin, Y. B. Ginat, A. P. Igoshev, and V. Desjacques, Axion resonances in binary pulsar systems, *J. Cosmology Astropart. Phys.* **2020**, 061 (2020), arXiv:1904.01958 [astro-ph.CO].
- [47] V. Desjacques, E. Grishin, and Y. B. Ginat, Axion Oscillations in Binary Systems: Angle-action Surgery, *ApJ* **901**, 85 (2020), arXiv:2003.10552 [gr-qc].
- [48] B. T. Chiang, H.-Y. Schive, and T. Chiueh, Soliton Oscillations and Revised Constraints from Eridanus II of Fuzzy Dark Matter, *Phys. Rev. D* **103**, 103019 (2021), arXiv:2104.13359 [astro-ph.CO].
- [49] R. C. Pantig and A. Övgün, Black Hole in Quantum Wave Dark Matter, *Fortschritte der Physik* **71**, 2200164 (2023), arXiv:2210.00523 [gr-qc].
- [50] D. J. E. Marsh, Axion cosmology, *Phys. Rep.* **643**, 1 (2016), arXiv:1510.07633 [astro-ph.CO].
- [51] P.-H. Chavanis, Mass-radius relation of Newtonian self-gravitating Bose-Einstein condensates with short-range interactions. I. Analytical results, *Phys. Rev. D* **84**, 043531 (2011), arXiv:1103.2050 [astro-ph.CO].
- [52] P.-H. Chavanis, Mass-radius relation of self-gravitating Bose-Einstein condensates with a central black hole, *European Physical Journal Plus* **134**, 352 (2019), arXiv:1909.04709 [gr-qc].
- [53] E. Y. Davies and P. Mocz, Fuzzy dark matter soliton cores around supermassive black holes, *MNRAS* **492**, 5721 (2020), arXiv:1908.04790 [astro-ph.GA].
- [54] D. Baumann, H. S. Chia, J. Stout, and L. ter Haar, The spectra of gravitational atoms, *J. Cosmology Astropart. Phys.* **2019**, 006 (2019), arXiv:1908.10370 [gr-qc].
- [55] R. Schödel, T. Ott, R. Genzel, R. Hofmann, M. Lehnert, A. Eckart, N. Mouawad, T. Alexander, M. J. Reid, R. Lenzen, *et al.*, A star in a 15.2-year orbit around the supermassive black hole at the centre of the Milky Way, *Nature* **419**, 694 (2002), arXiv:astro-ph/0210426 [astro-ph].
- [56] F. Eisenhauer, R. Genzel, T. Alexander, R. Abuter, T. Paumard, T. Ott, A. Gilbert, S. Gillessen, M. Horrobin, S. Trippe, *et al.*, SINFONI in the galactic center: Young stars and infrared flares in the central light-month, *The Astrophysical Journal* **628**, 246 (2005).
- [57] A. M. Ghez, S. Salim, S. D. Hornstein, A. Tanner, J. R. Lu, M. Morris, E. E. Becklin, and G. Duchêne, Stellar Orbits around the Galactic Center Black Hole, *ApJ* **620**, 744 (2005), arXiv:astro-ph/0306130 [astro-ph].
- [58] A. M. Ghez, S. Salim, N. N. Weinberg, J. R. Lu, T. Do, J. K. Dunn, K. Matthews, M. R. Morris, S. Yelda, E. E. Becklin, *et al.*, Measuring Distance and Properties of the Milky Way's Central Supermassive Black Hole with Stellar Orbits, *ApJ* **689**, 1044 (2008), arXiv:0808.2870 [astro-ph].
- [59] GRAVITY Collaboration, Abuter, R., Amorim, A., Anugu, N., Bauböck, M., Benisty, M., Berger, J. P., Blind, N., Bonnet, H., Brandner, W., *et al.*, Detection of the gravitational redshift in the orbit of the star s2 near the galactic centre massive black hole, *A&A* **615**, L15 (2018).
- [60] Event Horizon Telescope Collaboration, K. Akiyama, A. Alberdi, W. Alef, J. C. Algaba, R. Anantua, K. Asada, R. Azulay, U. Bach, A.-K. Baczko, *et al.*, First Sagittarius A* Event Horizon Telescope Results. I. The Shadow of the Supermassive Black Hole in the Center of the Milky Way, *ApJ* **930**, L12 (2022).
- [61] T. Panamarev, B. Shukirgaliyev, Y. Meiron, P. Berczik, A. Just, R. Spurzem, C. Omarov, and E. Vilko-viskij, Star-disc interaction in galactic nuclei: formation of a central stellar disc, *MNRAS* **476**, 4224 (2018), arXiv:1802.03027 [astro-ph.GA].
- [62] T. Panamarev, Y. B. Ginat, and B. Kocsis, Four-body problem in the angular momentum space, arXiv e-prints, arXiv:2507.10551 (2025), arXiv:2507.10551 [astro-ph.GA].
- [63] L. Hui, D. Kabat, X. Li, L. Santoni, and S. S. C. Wong, Black hole hair from scalar dark matter, *J. Cosmology Astropart. Phys.* **2019**, 038 (2019), arXiv:1904.12803 [gr-qc].
- [64] J. Bamber, K. Clough, P. G. Ferreira, L. Hui, and M. Lagos, Growth of accretion driven scalar hair around Kerr black holes, *Phys. Rev. D* **103**, 044059 (2021), arXiv:2011.07870 [gr-qc].
- [65] R. Schödel, D. Merritt, and A. Eckart, The nuclear star cluster of the Milky Way: proper motions and mass, *A&A* **502**, 91 (2009), arXiv:0902.3892 [astro-ph.GA].
- [66] P. J. E. Peebles, Origin of the Angular Momentum of Galaxies, *ApJ* **155**, 393 (1969).
- [67] J. S. Bullock, A. Dekel, T. S. Kolatt, A. V. Kravtsov, A. A. Klypin, C. Porciani, and J. R. Primack, A Universal Angular Momentum Profile for Galactic Halos, *ApJ* **555**, 240 (2001), arXiv:astro-ph/0011001 [astro-ph].
- [68] S. O. Schobesberger, T. Rindler-Daller, and P. R. Shapiro, Angular momentum and the absence of vortices in the cores of fuzzy dark matter haloes, *MNRAS* **505**, 802 (2021), arXiv:2101.04958 [astro-ph.GA].
- [69] A. Obreja, T. Buck, and A. V. Macciò, A first estimate of the Milky Way dark matter halo spin, *A&A* **657**, A15 (2022), arXiv:2110.11490 [astro-ph.GA].
- [70] H. J. Mo, S. Mao, and S. D. M. White, The formation of galactic discs, *MNRAS* **295**, 319 (1998), arXiv:astro-ph/9707093 [astro-ph].
- [71] M. Cautun, A. Benítez-Llambay, A. J. Deason, C. S. Frenk, A. Fattahi, F. A. Gómez, R. J. J. Grand, K. A. Oman, J. F. Navarro, and C. M. Simpson, The milky way total mass profile as inferred from Gaia DR2, *MNRAS* **494**, 4291 (2020), arXiv:1911.04557 [astro-ph.GA].

- [72] Y. B. Zel'Dovich, Generation of Waves by a Rotating Body, *Soviet Journal of Experimental and Theoretical Physics Letters* **14**, 180 (1971).
- [73] W. H. Press and S. A. Teukolsky, Floating Orbits, Superradiant Scattering and the Black-hole Bomb, *Nature* **238**, 211 (1972).
- [74] V. Cardoso, O. J. C. Dias, J. P. S. Lemos, and S. Yoshida, Black-hole bomb and superradiant instabilities, *Phys. Rev. D* **70**, 044039 (2004).
- [75] L. Šubr and J. Haas, Two-body Relaxation Driven Evolution of the Young Stellar Disk in the Galactic Center, *ApJ* **786**, 121 (2014), arXiv:1404.0380 [astro-ph.GA].
- [76] J. A. S. Hunt and E. Vasiliev, Milky Way dynamics in light of Gaia, arXiv e-prints, arXiv:2501.04075 (2025), arXiv:2501.04075 [astro-ph.GA].
- [77] A. Feldmeier, N. Neumayer, A. Seth, R. Schödel, N. Lützgendorf, P. T. de Zeeuw, M. Kissler-Patig, S. Nishiyama, and C. J. Walcher, Large scale kinematics and dynamical modelling of the Milky Way nuclear star cluster, *A&A* **570**, A2 (2014), arXiv:1406.2849 [astro-ph.GA].
- [78] L. D. Landau and E. M. Lifshitz, *Quantum mechanics*, third edition, revised and enlarged ed. (Pergamon Press, Oxford, 1989).
- [79] A. R. Edmonds, *Angular Momentum in Quantum Mechanics* (Princeton University Press, Princeton, N.J., 1960).
- [80] K. Clough, P. G. Ferreira, and M. Lagos, Growth of massive scalar hair around a Schwarzschild black hole, *Phys. Rev. D* **100**, 063014 (2019), arXiv:1904.12783 [gr-qc].
- [81] N. Bar, K. Blum, T. Lacroix, and P. Pani, Looking for ultralight dark matter near supermassive black holes, *J. Cosmology Astropart. Phys.* **2019**, 045 (2019), arXiv:1905.11745 [astro-ph.CO].
- [82] M. Born and V. Fock, Beweis des Adiabatenatzes, *Z. Phys.* **51**, 165 (1928).

General FDM Field

Potential. In this appendix we derive equation (8), for a general Bose–Einstein condensate gravitational atom. Let the axion field be

$$\psi(\mathbf{y}) = \sum_{n,l,m} \alpha_{nlm} R_{nl}(y) Y_{lm}(\hat{\mathbf{y}}), \quad (27)$$

where R_{nl} are the standard, hydrogen-atom radial wave-functions [78, §36], whence the density is

$$\rho(\mathbf{y}) = M_a \sum_{\substack{n_1, l_1, m_1, \\ n_2, l_2, m_2}} \alpha_{n_1 l_1 m_1} \alpha_{n_2 l_2 m_2}^* R_{n_1 l_1}(y) R_{n_2 l_2}^*(y) Y_{l_1 m_1}(\hat{\mathbf{y}}) Y_{l_2 m_2}^*(\hat{\mathbf{y}}). \quad (28)$$

Inserting this density and the spherical-harmonic decomposition of $|\mathbf{x} - \mathbf{y}|^{-1}$ in equation (7) into equation (5) gives an integral over a product of three spherical harmonics of $\hat{\mathbf{y}}$. Let us start, then, with this angular integral, over $\hat{\mathbf{y}}$, for each value of the quantum numbers $n_1, l_1, m_1, n_2, l_2, m_2$; this integral is [79]

$$\int d^2 \hat{\mathbf{y}} Y_{lm}(\hat{\mathbf{y}}) Y_{l_1 m_1}(\hat{\mathbf{y}}) Y_{l_2 m_2}^*(\hat{\mathbf{y}}) = (-1)^{m_2} \int d^2 \hat{\mathbf{y}} Y_{lm}(\hat{\mathbf{y}}) Y_{l_1 m_1}(\hat{\mathbf{y}}) Y_{l_2, -m_2}(\hat{\mathbf{y}}) \quad (29)$$

$$= (-1)^{m_2} \sqrt{\frac{(2l+1)(2l_1+1)(2l_2+1)}{4\pi}} \begin{pmatrix} l & l_1 & l_2 \\ 0 & 0 & 0 \end{pmatrix} \begin{pmatrix} l & l_1 & l_2 \\ m & m_1 & -m_2 \end{pmatrix}, \quad (30)$$

where $\begin{pmatrix} l_3 & l_2 & l_1 \\ m_3 & m_2 & m_1 \end{pmatrix}$ is the 3- j symbol (which vanishes for $m_1 + m_2 + m_3 \neq 0$).

Inserting this into the potential $\Phi(\mathbf{x})$ in equation (5) gives

$$\begin{aligned} \Phi(\mathbf{x}) = & GM_a \sum_{\substack{l,m, \\ n_1, l_1, m_1, \\ n_2, l_2, m_2}} (-1)^{m_2+1} \sqrt{\frac{4\pi(2l_1+1)(2l_2+1)}{(2l+1)}} \begin{pmatrix} l & l_1 & l_2 \\ 0 & 0 & 0 \end{pmatrix} \begin{pmatrix} l & l_1 & l_2 \\ m & m_1 & -m_2 \end{pmatrix} \\ & \times \alpha_{n_1 l_1 m_1} \alpha_{n_2 l_2 m_2}^* \int_0^\infty dy y^2 R_{n_1 l_1}(y) R_{n_2 l_2}(y) Y_{lm}^*(\hat{\mathbf{x}}) \frac{\min\{x, y\}^l}{\max\{x, y\}^{l+1}}. \end{aligned} \quad (31)$$

This expression, while analytical, is too complicated to be of practical use. Let us now double-average it over the mean anomaly and the argument of pericentre, where \mathbf{x} performs of a Keplerian orbit about the origin. The problem is that, as $|\psi\rangle$ is written in a specific basis, which comes with a specific co-ordinate system—a choice of a $\hat{\mathbf{z}}$ axis for

the gravitational atom—we are not free to choose the direction of $\hat{\mathbf{x}}$. But, if $R = R(i, \Omega, \omega)$ is a rotation matrix which transforms the orbit from the $\hat{\mathbf{x}}\text{-}\hat{\mathbf{y}}$ plane to the reference frame used here, then by virtue of the spherical harmonics being an irreducible representation of $SO(3)$,

$$Y_{lm}^*(\hat{\mathbf{x}}) = \sum_{m'=-l}^l \left[D_{mm'}^{(l)}(R) \right] Y_{lm'}^*(\hat{\mathbf{x}}'), \quad (32)$$

where now $\hat{\mathbf{x}}'$ is in the $\hat{\mathbf{x}}\text{-}\hat{\mathbf{y}}$ plane, and $D(R)$ is Wigner's D-matrix [79].

Now, that $\hat{\mathbf{x}}'$ is oriented properly, the only terms affected by orbit-averaging are $Y_{lm'}^*(\hat{\mathbf{x}}') \min\{x, y\}^l / \max\{x, y\}^{l+1}$, because the D-matrix only depends on i, Ω and ω , which are fixed along an orbit. Indeed, the average

$$\left\langle \frac{\min\{x, y\}^l}{\max\{x, y\}^{l+1}} Y_{lm'}^*(\hat{\mathbf{x}}') \right\rangle_{\text{da}} \quad (33)$$

is equivalent to the double-average of a VRR interaction where one of the stars (with position \mathbf{y}) has a circular orbit. This is therefore completely equivalent to a two-ring interaction, which, fortunately, was already treated by ref. [19]. The result is

$$\left\langle \frac{\min\{x, y\}^l}{\max\{x, y\}^{l+1}} Y_{lm'}^*(\hat{\mathbf{x}}')^* D_{mm'}^{(l)}(R) \right\rangle_{\text{da}} = \frac{\sqrt{2l+1}}{\sqrt{4\pi} \max\{a, y\}} P_l(0) \delta^K(m', 0) \left[\frac{\min\{a, y\}}{\max\{a, y\}} \right]^l s_l(a, y, e, 0) D_{m0}^{(l)}(R), \quad (34)$$

where δ^K is the Kronecker delta-function, and s_l is defined in ref. [19], and its value depends on whether $y < a(1-e)$, $a(1-e) \leq y \leq a(1+e)$, or $y > a(1+e)$.

Setting $m' = 0$ because of the delta-function also simplifies the D-matrix greatly, since

$$D_{m0}^{(l)}(R) = \sqrt{\frac{4\pi}{2l+1}} Y_{lm}^*(i, \Omega), \quad (35)$$

whence equation (31) yields equation (8), *viz.*,

$$\langle \Phi \rangle_{\text{da}} = - \sum_{l,m} J_{lm} Y_{lm}^*(\hat{\mathbf{L}}), \quad (36)$$

where

$$\begin{aligned} J_{lm} = & GM_a \sum_{\substack{n_1, l_1, m_1, \\ n_2, l_2, m_2}} (-1)^{m_2} \sqrt{\frac{4\pi(2l_1+1)(2l_2+1)}{(2l+1)}} P_l(0) \begin{pmatrix} l & l_1 & l_2 \\ 0 & 0 & 0 \end{pmatrix} \begin{pmatrix} l & l_1 & l_2 \\ m & m_1 & -m_2 \end{pmatrix} \\ & \times \alpha_{n_1 l_1 m_1} \alpha_{n_2 l_2 m_2}^* \int_0^\infty dy \frac{y^2 R_{n_1 l_1}(y) R_{n_2 l_2}(y)}{\max\{a, y\}} \left[\frac{\min\{a, y\}}{\max\{a, y\}} \right]^l s_l(a, y, e, 0). \end{aligned} \quad (37)$$

By the properties of the 3- j symbol, the only non-zero contributions to J_{lm} are from $m_2 = m + m_1$ and $|l_1 - l_2| \leq l \leq l_1 + l_2$. For instance, this implies that if $|\psi\rangle$ is an eigenstate $|n_0, l_0, m_0\rangle$, then $\langle \Phi \rangle_{\text{da}}$ only has terms with $m = 0$ and $l \in \{0, \dots, 2l_0\}$. Then, equation (37) yields

$$\frac{J_{l, l_0}}{GM_a} = (-1)^{m_0} (2l_0 + 1) P_l(0) \begin{pmatrix} l & l_0 & l_0 \\ 0 & 0 & 0 \end{pmatrix} \begin{pmatrix} l & l_0 & l_0 \\ 0 & m_0 & -m_0 \end{pmatrix} |\alpha_{n_0 l_0 m_0}|^2 \int_0^\infty dy \frac{y^2 R_{n_0 l_0}^2(y)}{\max\{a, y\}} \left[\frac{\min\{a, y\}}{\max\{a, y\}} \right]^l s_l(a, y, e, 0). \quad (38)$$

We remark, that the energy levels of the gravitational atom are such that the frequencies are [54]

$$\omega_{nlm} = \frac{E_{nlm}}{\hbar} \approx \frac{G^2 M_\bullet^2 m_a^3}{2n^2 \hbar^2} \gg \text{Myr}^{-1} \quad (39)$$

for order-unity n , so in-so-far as VRR is concerned, orbit-averaging should remove the quantum interference between different energy-levels, i.e. set $\alpha_{n_1 l_1 m_1} \alpha_{n_2 l_2 m_2}^* \mapsto 0$ in (37) if $n_1 \neq n_2$.

Accretion and super-radiant instability. If $m_a \gtrsim 10^{-18}$ eV, then the time-scale for the super-radiant instability for the most unstable mode $|211\rangle$ is much shorter than a Hubble time, for $M_\bullet = 4 \times 10^6 M_\odot$, whence for $m_a \gtrsim 10^{-18}$ eV, $|\psi\rangle$ would be dominated by the fastest-growing super-radiant mode. However, as seen in figures 2 and 4, the constraints from the nuclear stellar disc are much stronger when $m_a < 10^{-18}$ eV, even though in this case the instability's growth rate is too slow to matter, even over a Hubble time. We thus keep α and M_a as given by equations (17) and (21), rather than $\alpha = 1$ (as would be the case for $m_a \gtrsim 10^{-18}$ eV).

Note, that the $l = 0$ modes of the soliton might be accreted by the SMBH, thereby weakening constraints from mass precession [53, 63, 64, 80, 81]: the decay rate due to accretion (conversely, the growth-rate of the super-radiant instability) of mode $|nlm\rangle$ is [54]

$$\Gamma_{nlm} \sim (m\Omega_\bullet - \omega_{nlm}) \left(\frac{GM_\bullet m_a}{\hbar c} \right)^{4l+5}, \quad (40)$$

where $\omega_{nlm} = E_{nlm}/\hbar$ is the oscillation frequency of this mode, $\Omega_\bullet \equiv c^3 \chi_\bullet \left[4GM_\bullet \left(1 + \sqrt{1 - \chi_\bullet^2} \right) \right]^{-1} \gg \omega_{nlm}$, and χ_\bullet is the dimension-less spin of the SMBH. This implies that, for $l = 0$, Γ_{n00}^{-1} is of the order of the age of the Universe (or smaller) for spherically symmetric modes, $M_\bullet = 4 \times 10^6 M_\odot$ and $m_a \gtrsim 5 \times 10^{-20}$ eV; but the $l \neq 0$ modes, with which we are concerned here, are protected by the extra power of $4l$, and hence their accretion time-scale is far longer than a Hubble time for $m_a < 10^{-18}$ eV.

Wave-function shape. Let us give an argument for equation (20). Let us first consider the case where the soliton forms during halo formation, and the SMBH grows adiabatically as the Galaxy evolves. In that case, initially, well inside the core, the gravitational potential is that of a 3D harmonic oscillator, where the energy levels grow linearly with n . Thus, the total energy is roughly $E_0 \left[1 - |\alpha|^2 + (n-1)|\alpha|^2 \right]$, where E_0 is the ground-state energy. If $|\alpha|^2 \sim 1/l$ (cf. equation (21)), with $l \leq n-1$, then the total energy is approximately independent of l . This neglects the self-gravity of the $l \neq 0$ modes, which, when accounted for, would increase the energy by a term proportional to $|\alpha|^4 \left(1 - \frac{\langle r \rangle_{n=1}}{\langle \psi | r | \psi \rangle} \right)$, which is minimised by taking ψ to include just the lowest possible states n with $l \neq 0$, i.e. only $n = 1, 2$, with the magnitude of the ($n = 2, l = 1$) component fixed by the angular-momentum constraint. This is without an SMBH, but by the adiabatic theorem [82], this state would evolve into equation (20) as the SMBH grows.

Let us now consider the opposite case, where the soliton forms with the SMBH *in situ*. Let $|\psi\rangle \propto \alpha_{n_1 0 0} |n_1 0 0\rangle + \sum_{l_0 m_0} \alpha_{n_0 l_0 m_0} |n_0 l_0 m_0\rangle$, where $l_0 \neq 0$. The spherically symmetric $|n_1 0 0\rangle$ component will be accreted onto the SMBH, leaving only the states $|n_0 l_0 m_0\rangle$. Such a state has the lowest energy if n_0 is lowest, but for $l_0 \neq 0$, this requires $n_0 \geq 2$, with the minimum energy achieved by $n_0 = 2$, whence $l_0 = 1$. We assume that the system would relax to this state. If we orient the $\hat{\mathbf{z}}$ axis to align with the direction of $\langle \mathbf{L}_a \rangle$, then the conditions that $\langle L_{a,x} \rangle = \langle L_{a,y} \rangle = 0$ and $\langle L_{a,z} \rangle > 0$ fix $\alpha_{n_0 l_0 0} = 0$. If $\langle L_{a,z} \rangle$ is fixed, then so is $|\alpha_{211}|^2 - |\alpha_{21-1}|^2$. Minimising $|\alpha|^2 = |\alpha_{211}|^2 + |\alpha_{21-1}|^2$, subject to this constraint (to minimise the total energy), yields $\alpha_{21-1} = 0$, $\alpha_{211} = \alpha$. Hence equation (20) arises in both cases.